PERGAMON

International Journal of Solids and Structures 39 (2002) 3997–4011

INTERNATIONAL JOURNAL OF SOLIDS and STRUCTURES

www.elsevier.com/locate/ijsolstr

Nonlinear magnetoelastic coupling effects in a soft ferromagnetic material with a crack

Wei Liang [a,*], Daining Fang [a], Yapeng Shen [b], Ai Kah Soh [c]

[a] *Department of Engineering Mechanics, Tsinghua University, Beijing 100084, China*
[b] *The State Key Laboratory of Mechanical Structural Strength and Vibration, Xi'an Jiaotong University, Xi'an 710049, China*
[c] *Department of Mechanical Engineering, University of Hong Kong, Hong Kong, China*

Received 11 October 2001

Abstract

In this paper, the magnetoelastic coupling effect in an infinite soft ferromagnetic material with a crack is analyzed. The nonlinear effect of magnetic field upon stress and the effect of the deformed crack configuration are taken into consideration. The coupling field is determined in the deformed configuration by regarding the deformed crack as an elliptical cylinder with its geometric coefficients, which are determined from a set of algebraic equations deduced from the displacements. The magnetic and stress fields near the crack tip are discussed for the case where both of the magnetic loading and the mechanical tension are present.

Keywords: Magnetoelasticity; Nonlinearity; Deformed crack

1. Introduction

In recent years, there is a growing interest among researchers (Shindo, 1977, 1980; Moon, 1984; Yeh, 1989; Sabir and Maugin, 1996; Shindo et al., 1997, 2000; Bagdasarian and Hasanian, 2000; Clatterbuck et al., 2000) in solving fracture problems of magnetoelasticity, which has important applications in non-destructive testing and the design of smart materials. Shindo (1977, 1980) has established closed form solutions for linear problems of cracks in soft ferromagnetic materials. Yeh (1989) analyzed the magnetic field generated by mechanical singularity in a half plane. Sabir and Maugin (1996) performed analytical work of the conservation integral in ferromagnetic materials. The linear magneto-elasticity solution of wave scattering at a through crack in conducting plates subjected to a uniform magnetic field was obtained by Shindo et al. (1997, 2000). Bagdasarian and Hasanian (2000) has performed the analysis of the soft ferromagnetic elastic half plane with a crack. Clatterbuck et al. (2000) carried out experiments to determine the fracture toughness of Incoloy 908. In the analysis of magnetoelastic problems, the linearized models proposed by Pao and Yeh (1973) and Eringen (1989) were widely used. That is, the magnetic field was

* Corresponding author. Fax: +86-10-62773779.
E-mail address: weiliang@tsinghua.edu.cn (W. Liang).

PII: S0020-7683(02)00266-4

regarded as a linear sum of the quantity in the rigid body and a perturbation quantity due to deformation based on such an assumption that the perturbation part is comparatively very small. However, since the concentration of magnetic field near a crack is significant, at most cases, to keep the presupposition of the linearized model may be inappropriate and the nonlinear relation between the stress and the magnetic field needs to be considered.

For coupling field problems, Shindo (1977) has observed that the difference between the deformed and undeformed crack surface boundary conditions could not be directly neglected. This is because the small difference multiplied by a large relative permeability may no longer be very small. With the rapid advancement of research on piezoelectric materials with defects, the effect of the difference between the deformed and undeformed cracks on fracture of the coupling field was investigated. Sosa and Khutoryansky (1996) obtained the exact electric boundary conditions by considering a hole. McMeeking (1999, 2001) investigated the electric field by taking the deformed crack surface into consideration. In the work of Zhang (1998) and Zhang et al. (1998) the electric field influenced by deformed crack face was considered.

In this paper, a general solution of a magnetoelastic plane, for which the nonlinear effect of the magnetic field on stresses is considered, is obtained in terms of complex functions. The deformed crack surface is identified by means of the displacements. The coupling field is analytically determined. The shape of the deformed crack surface and the field near the crack tip will be discussed.

2. Basic equations of static magnetoelasticity

The general theory on the behavior of deformable ferromagnetic materials in magnetic field was established based on electrodynamics and mechanics of continuum (Brown, 1966; Eringen, 1980; Maugin, 1988). For the analysis of soft ferromagnetic materials with multi-domain structures, the commonly made assumptions are that the magnetic hysteresis and magnetostrictive effect are negligible and the magnetization relation is linear before saturation (Wohlfarth, 1980). The fundamental equations for solving quasi-static magnetoelastic problems consist of Biot–Savart Law, Ampere Law and Cauchy's equations for the equilibrium of linear and angular momenta in the Euler coordinates. Based on Brown' model of magnetic force, the field equations are given as follows (Pao and Yeh, 1973; Moon, 1984; Yerma and Singh, 1984):

$$\begin{aligned} &b_{i,i} = 0, \qquad e_{ijk}h_{j,k} = 0 \\ &t_{ij,i} + \mu_0 m_k h_{j,k} = 0, \quad e_{ijk}t_{jk} + \mu_0 e_{ijk} m_j h_k = 0 \end{aligned} \tag{1}$$

where b_i, m_i and h_i are the magnetic induction, magnetization and magnetic field vectors; $\mu_0 (= 4\pi \times 10^{-7}\ \mathrm{N/A^2})$ is the permeability of vacuum; e_{ijk} is a permutation tensor and comma in Eq. (1) denotes partial derivative with respect to the spatial variables; and t_{ij} is the magnetoelastic stress tensor, which expresses the tractions on the surface of an infinitesimal element caused by both the elastic effect and magnetic field.

On the boundary surface of the magnetic body, the equation of equilibrium of motion requires the continuity conditions of stress and magnetic field to be satisfied. The continuity conditions in the equilibrium state can be expressed (Moon, 1984) as follows:

$$n_i[[t_{ij} + t_{ij}^{\mathrm{M}}]] = 0, \quad n_i[[b_i]] = 0, \quad e_{ijk}n_j[[h_k]] = 0 \tag{2}$$

where n_i is the unit normal vector of the surface in the equilibrium state; $[[\cdot]]$ denotes the jump of the quantity through the material interval; and t_{ij}^{M} is Maxwell stress tensor, i.e., $t_{ij}^{\mathrm{M}} = b_i h_j - \frac{1}{2}\mu_0 h_k h_k \delta_{ij}$. In general, the motion between a reference configuration, K_R, which is free of loads, and the current configuration, K_t, at time, t, is presented by means of the following mapping of Euclidean space:

$$x_i = x_i(X_K, t), \quad i = 1, 2, 3, \ \ K = 1, 2, 3 \tag{3}$$

where x_i are the Eulerian coordinates and X_K are material coordinates. The displacement field can be expressed as

$$u_i = x_i - \delta_{iK}X_K + d_k \quad \text{or} \quad U_K = \delta_{Ki}x_i - X_K + D_K \tag{4}$$

where u_i and U_K are the displacements in the current and reference configurations, respectively; δ_{Ki} are the shift tensors of the coordinate systems; d_k and D_k represent the displacement between the origin points of the two coordinates.

By assuming small deformation, i.e., $|x_{i,K}| \ll 1$, the geometric relations can be reduced. The difference of stresses in different configurations can be indifferent just like in the case of elasticity. The boundary in the deformed equilibrium state is different from that in the undeformed configuration. In dealing with a noncoupling elastic problem, the difference can be neglected based on the assumption of small deformation. However, in the case of the magnetoelastic problem, the small difference of vectors multiplied by a large number of susceptibility may be not very small (Shindo, 1977). Therefore, the difference between the boundary in the deformed configuration and that in the undeformed configuration should not be simply neglected even if the deformation is small.

The constitutive equations for isotropic soft ferromagnetic materials can be expressed as (Pao and Yeh, 1973)

$$t_{ij} = \sigma_{ij} + \mu_0 m_j h_i, \quad \sigma_{ij} = \lambda u_{k,k}\delta_{ij} + G(u_{i,j} + u_{j,i}), \quad m_i = \chi h_i \tag{5}$$

where λ and G are Lame constants and χ is the magnetic susceptibility of the material; δ_{ij} are Kronecker symbols.

3. The general solution for plane magnetoelastic problems

Consider a soft ferromagnetic material subjected to a static magnetic field and a mechanical load, which are applied in-plane. The problem can be regarded as a plane problem. From Eqs. (1), (2) and (5), the third expression of Eq. (1) can be rewritten as

$$\begin{aligned} &\frac{\partial\sigma_{xx}}{\partial x} + \frac{\partial\sigma_{xy}}{\partial y} - (-\mu_0\chi)\left(\frac{\partial h_x^2}{\partial x} + \frac{\partial h_y^2}{\partial x}\right) = 0 \\ &\frac{\partial\sigma_{yx}}{\partial x} + \frac{\partial\sigma_{yy}}{\partial y} - (-\mu_0\chi)\left(\frac{\partial h_x^2}{\partial y} + \frac{\partial h_y^2}{\partial y}\right) = 0 \end{aligned} \tag{6}$$

Thus, the solution of the field Eq. (1) can be expressed in terms of the magnetic scalar potential, $\xi(x, y)$, and stress function, $U(x, y)$, as follows:

$$\begin{aligned} &\sigma_{ij} = U_{,ij} - \nabla U - \mu_0\chi\delta_{ij}(h_k h_k) \\ &h_i = \xi_{,i} \end{aligned} \tag{7}$$

and

$$\nabla^2\xi = 0 \tag{8}$$

To insure the existence of single-valued displacements, the equation of compatibility is required. Making use of Eqs. (7) and (8), the equation of compatibility can be expressed as

$$\nabla^2\nabla^2 U = -\nabla^2\big(-\mu_0\chi(1 - v)\xi_{,k}\xi_{,k}\big) \tag{9}$$

where v is the Poisson's ratio of the plane problem.

Thus, Eqs. (8) and (9) are the governing equations of the plane magnetoelastic problem. The solution of the governing equations can be expressed in terms of analytic functions. By following a procedure similar to that described by Knops (1963), the stress, magnetic and displacement fields can be expressed as

$$\begin{aligned}
&\sigma_{xx} + \sigma_{yy} = 2\left(\varphi'(z) + \bar{\varphi}'(\bar{z})\right) + \mu_1\omega'(z)\bar{\omega}'(\bar{z}) \\
&\sigma_{yy} - \sigma_{xx} + 2\mathrm{i}\sigma_{xy} = 2\left(\bar{z}\varphi''(z) + \psi'(z)\right) - \mu_2\omega''(z)\bar{\omega}(\bar{z}) \\
&h_x - \mathrm{i}h_y = \omega'(z) \\
&2G(u_x + \mathrm{i}u_y) = \kappa\varphi(z) - z\bar{\varphi}'(\bar{z}) - \bar{\psi}(\bar{z}) - \tfrac{1}{2}\mu_2\omega(z)\bar{\omega}'(\bar{z})
\end{aligned} \tag{10}$$

where $z = x + \mathrm{i}y$ and $\varphi(z)$, $\psi(z)$, $\omega(z)$ are complex potentials. In the case of plane stress, $\kappa = (3 - v)/(1 + v)$, and for the case of plane strain, $\kappa = (3 - 4v)$. The constant

$$\mu_1 = -\mu_0\chi(1 + v), \quad \mu_2 = -\mu_0\chi(1 - v) \tag{11}$$

Making use of Eqs. (2) and (10), the continuity conditions of the stress and magnetic fields on the boundary surface of the ferromagnetic material can be expressed as

$$\begin{aligned}
&\mathrm{Re}\,\omega(z) = \mathrm{Re}\,\omega_-(z) \\
&(\chi + 1)\mathrm{Re}[(n_1 + \mathrm{i}n_2)\omega'(z)] = (\chi_- + 1)\mathrm{Re}[(n_1 + \mathrm{i}n_2)\omega'_-(z)] \\
&n_i t^b_{ij} = \overline{X}_j
\end{aligned} \tag{12}$$

where $\boldsymbol{n} = (n_1, n_2)$ is the unit normal vector of the deformed surface; the subscript minus, "$_-$", denotes the magnetic quantities outside the surface; and $\overline{X}_i$ is the mechanical traction on the surface. The tensor t^b_{ij} is given by

$$\begin{aligned}
&t^b_{xx} + t^b_{yy} = 2\left(\varphi'(z) + \bar{\varphi}'(\bar{z})\right) + (1 - v)\mu_0\chi\omega'(z)\bar{\omega}'(\bar{z}) - 2\mu_0\chi_-\omega'_-(z)\bar{\omega}'_-(\bar{z}) \\
&t^b_{yy} - t^b_{xx} + 2\mathrm{i}t^b_{xy} = 2\left(\bar{z}\varphi''(z) + \psi'(z)\right) + (1 - v)\mu_0\chi\omega''(z)\bar{\omega}(\bar{z}) - \mu_0(2\chi + 1)\omega'(z)^2 \\
&\qquad - (1 - v_-)\mu_0\chi_-\omega''_-(z)\bar{\omega}_-(\bar{z}) + \mu_0(2\chi_- + 1)\omega'_-(z)^2
\end{aligned} \tag{13}$$

which are determined in terms of the stress inside the body and the magnetic field both inside and outside the body.

4. The crack problem

Fig. 1 shows a crack of length $2a$ in an infinite soft ferromagnetic elastic plate, subjected to an in-plane magnetic field $\boldsymbol{b}_0$ and a mechanical tension $\boldsymbol{p}$, which causes the crack to open after deformation. Let $X'Y'$ be the material coordinate system and the X'-axis is along the undeformed crack line. θ_b and θ_p indicate the direction of $\boldsymbol{b}_0$ and $\boldsymbol{p}$, respectively. In the original configuration, two overlapped line segments represent the crack surface, which becomes a closed curved surface after deformation. In an elastic problem, the deformed crack surface is an elliptical cylinder. The opening of the deformed crack is very small. Moreover, the linear magnetoelastic analysis of crack problems shows that the displacement induced by magnetic loading is less than that by mechanical loading. Thus, the deformed crack surface of magnetoelasticity can be considered as is an elliptical cylinder. Assume that γ denotes the projection of the deformed crack face on the $X'Y'$ plane. Due to the fact that the problem is centrosymmetric, three undetermined geometric coefficients are needed to depict the curve γ. These coefficients are the semi-axes of the ellipse, α and β, and the angle from the undeformed crack line to the major principle axis, ϑ. For small deformation, β/α is very

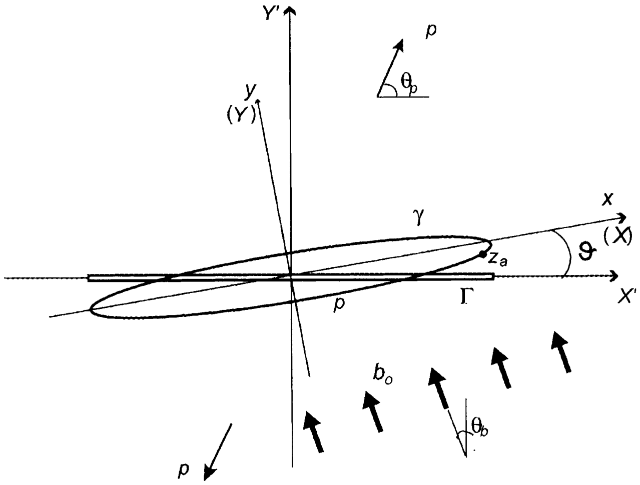

Fig. 1. Schematic of the problem: an infinite soft ferromagnetic medium with a crack subject to in-plane tension and magnetic field.

small. Note that xy is the space coordinate system, and the x-axis is in the same direction as the principle axis of the deformed crack surface. In general, the pole of the ellipse may not be the same as the material point of the crack tip in the undeformed configuration. The position of the crack tip in the deformed configuration is indicated as z_a. The complex valuable $z = x + \mathrm{i}y$ is defined in the xy coordinate system. To obtain the complex functions, $\varphi(z)$, $\psi(z)$ and $\omega(z)$ in Eq. (10), the conditions of the homogeneous field far from the crack and the boundary conditions on the crack surface are needed.

The homogeneous magnetic and stress fields are given by

$$\begin{aligned} &\sigma^{\infty}_{X'X'} + \sigma^{\infty}_{Y'Y'} = p \\ &\sigma^{\infty}_{Y'Y'} - \sigma^{\infty}_{X'X'} + 2\mathrm{i}\sigma^{\infty}_{X'Y'} = -p\exp(-2\mathrm{i}\theta_p) \\ &h^{\infty}_{X'} + \mathrm{i}h^{\infty}_{Y'} = b_0 \exp(\mathrm{i}(\theta_b + \tfrac{1}{2}\pi))/(\mu_0(1+\chi)) \end{aligned} \tag{14}$$

where σ^{∞}_{ij} and h^{∞}_i denote the remote stress and magnetic field. b_0 and p represent the applied magnetic field and the mechanical tension, respectively; and the corresponding directions are θ_p and θ_b.

Since the deformed crack is open, the medium inside the crack is assumed to have magnetic susceptibility χ_-. The crack surface is free of mechanical traction. From Eqs. (12) and (13), the boundary conditions on the deformed crack surface can be expressed as

$$\begin{aligned} &\mathrm{Re}[(n_2 - \mathrm{i}n_1)\omega'(z)] = \mathrm{Re}[(n_2 - \mathrm{i}n_1)\omega'_-(z)] \\ &(\chi+1)\mathrm{Re}[(n_1 + \mathrm{i}n_2)\omega'(z)] = (\chi_- + 1)\mathrm{Re}[(n_1 + \mathrm{i}n_2)\omega'_-(z)], \qquad z \in \gamma \\ &\left[\varphi(z) + z\bar{\varphi}'(\bar{z}) + \bar{\psi}(\bar{z}) + \mu_2\omega(z)\bar{\omega}'(\bar{z}) - \mu_3\bar{s}(\bar{z}) + \mu_4\omega_-(z)\bar{\omega}'_-(\bar{z}) + \mu_5\bar{s}_-(\bar{z})\right]_{P_2}^{P_1} = 0 \end{aligned} \tag{15}$$

where P_1 and P_2 are two points on γ. $s(z)$ is a function defined by

$$s(z) = \int \omega'(z)^2\,\mathrm{d}z, \quad s_-(z) = \int \omega'_-(z)^2\,\mathrm{d}z \tag{16}$$

The constants are

$$\mu_3 = \mu_0(\chi + \tfrac{1}{2}), \quad \mu_4 = \mu_0\chi_-(1 - \nu_-), \quad \mu_5 = \mu_0(\chi_- + \tfrac{1}{2}) \tag{17}$$

5. Solution of the coupling field

Since the region is multiply connected, the multi-valuedness of the complex functions needs to be considered. From the third expression of Eq. (10), the first and second continuity conditions of Eq. (15) and the single valuedness of magnetic intensity, the functions $\omega(z)$ and $\omega_-(z)$ can be determined to be the single valued. They can be expressed in Lauren series as follows:

$$\omega(z) = C_1 z + \sum_{k=1}^{\infty} C_{-k} z^{-k}, \quad \omega_-(z) = \sum_{k=1}^{\infty} F_k z^k \tag{18}$$

From the first, second and fourth expressions of Eq. (10) and the last expression of Eq. (15), one can deduce that the single valuedness of stresses and displacements requires that the multi-valuedness of $\varphi(z)$ and $\psi(z)$ be dependent on the characteristics of functions $S(z)$ and $S_-(z)$. However, $S(z)$ and $S_-(z)$ can be determined to be holomorphic in their analytic regions from Eqs. (16) and (18). Thus $\varphi(z)$ and $\psi(z)$ can be represented by

$$\varphi(z) = A_1 z + \sum_{k=1}^{\infty} A_{-k} z^{-k}, \quad \psi(z) = B_1 z + \sum_{k=1}^{\infty} B_{-k} z^{-k} \tag{19}$$

Note that the series employed in Eqs. (18) and (19) are chosen such that the physical quantities at infinity are finite. Moreover, from Eq. (14), it can be deduced that

$$\begin{aligned} A_1 &= \tfrac{1}{4} p, \\ B_1 &= -\tfrac{1}{2} p \exp(-2\mathrm{i}\theta_p + 2\mathrm{i}\vartheta), \\ \overline{C}_1 &= b_0 \exp(\mathrm{i}(\theta_b + \tfrac{1}{2}\pi - \vartheta))/(\mu_0(\chi + 1)) \end{aligned} \tag{20}$$

The following conformal transformation,

$$z = g(\zeta) = R(\zeta + m\zeta^{-1}) \tag{21}$$

can be used to solve Eq. (15). Note that m and R are also geometric parameters of γ. These two parameters are related to the undetermined coefficients α and β as follows:

$$m = \frac{(\alpha - \beta)}{\alpha + \beta}, \quad R = \tfrac{1}{2}(\alpha + \beta) \tag{22}$$

where $0 \leqslant m \leqslant 1$ and it can be determined that $(1 - m)$ is a quantity as small as α/β.

Thus, the complex potentials can be written as

$$\begin{aligned} \varphi(z) &= \Phi(\zeta) = RA_1\zeta + \Phi_0(\zeta) \\ \psi(z) &= \Psi(\zeta) = RB_1\zeta + \Psi_0(\zeta) \\ \omega(z) &= W_0(\zeta) = RC_1\zeta + W_0(\zeta) \\ \omega_-(z) &= W_-(\zeta) = RF(\zeta + m\zeta^{-1}) \end{aligned} \tag{23}$$

where $\varphi(z) = \Phi(\zeta)$, $\psi(z) = \Psi(\zeta)$, $\omega(z) = W_0(\zeta)$, $\omega_-(z) = W_-(\zeta)$. $W_0(z)$, $\Phi_0(\zeta)$ and $\Psi_0(z)$ are holomorphic functions in the region where $|\zeta| > 1$. These functions can be expressed in series as follows:

$$W_0(\zeta) = R\sum_{k=1}^{\infty} c_{-k}\zeta^{-k}, \quad \Phi_0(\zeta) = \sum_{k=1}^{\infty} a_{-k}\zeta^{-k}, \quad \Psi_0(\zeta) = \sum_{k=1}^{\infty} b^*_{-k}\zeta^{-k} \tag{24}$$

By using Eq. (23), Eq. (15) can be re-written as follows:

$$
\begin{aligned}
&W(\sigma)+\overline{W}(\sigma^{-1})=W_{-}(\sigma)+\overline{W}_{-}(\sigma^{-1})\\
&(\chi+1)(W(\sigma)-\overline{W}(\sigma^{-1}))=W_{-}(\sigma)-\overline{W}_{-}(\sigma^{-1})\\
&\Phi(\sigma)+\frac{g(\sigma)}{\overline{g}'(\sigma^{-1})}\overline{\Phi}'(\sigma^{-1})+\overline{\Psi}(\sigma^{-1})+\frac{\mu_2 W(\sigma)\overline{W}'(\sigma^{-1})}{\overline{g}'(\sigma^{-1})}-\mu_3\overline{S}(\sigma^{-1})+\frac{\mu_4 W_{-}(\sigma)\overline{W}'_{-}(\sigma^{-1})}{\overline{g}'(\sigma^{-1})}+\mu_5\overline{S}_{-}(\sigma^{-1})=0
\end{aligned}
\tag{25}
$$

where $\sigma=e^{i\theta}$. The functions, $S(\zeta)$ and $S_{-}(\zeta)$, are obtained from the following relation deduced from Eq. (16)

$$
\frac{S'(\zeta)}{g'(z)}=\frac{W'(\zeta)^2}{g'(z)^2}\quad\text{or}\quad S(\zeta')=\int\frac{W'(\zeta)^2}{g'(\zeta)}\,d\zeta
\tag{26}
$$

By using Cauchy integral method, we can obtain through solving Eq. (25)

$$
\begin{aligned}
&W(\zeta)=RC_1\zeta+Rc_{-1}\zeta^{-1}\\
&\Phi(z)=RA_1\zeta+a_{-1}\zeta^{-1}\\
&\Psi(\zeta)=R\Bigg(B_1\zeta-(\overline{A}_1+\mu_3Rc_{-1}^2m^{-1}+\mu_4F\overline{F}+\mu_5F^2m)\zeta^{-1}\\
&\qquad-\frac{(\zeta+m\zeta^{-1})(A_1-R^{-1}a_{-1}\zeta^{-2})-\mu_2((C_1\overline{C}_1-c_{-1}\bar{c}_{-1})\zeta^{-1}-\overline{C}_1c_{-1}\zeta^{-3}+C_1\bar{c}_{-1}\zeta)}{1-m\zeta^{-2}}\\
&\qquad-\frac{(1+m)A_1\zeta}{\zeta^2-m}+\eta(\zeta,m)+C_S\Bigg)
\end{aligned}
\tag{27}
$$

where C_S is an integral constant from Eq. (26), which can be determined by setting the rigid body displacement to zero. The coefficients a_{-1}, c_{-1} and F are related to the applied magnetic field and mechanical tension, that is

$$
\begin{aligned}
&a_{-1}=-R\left(\overline{A}_1m+\overline{B}_1+\mu_2C_1\bar{c}_{-1}-\mu_3\overline{C}_1^2+\mu_4F\overline{F}m+\mu_5\overline{F}^2\right)\\
&c_{-1}=\frac{2m+\chi(1+m)}{2+\chi(1+m)}\operatorname{Re}C_1+i\frac{2m-\chi(1-m)}{2+\chi(1-m)}\operatorname{Im}C_1\\
&F=\frac{2(1+\chi)}{2+\chi(1+m)}\operatorname{Re}C_1+i\frac{2(1+\chi)}{2+\chi(1-m)}\operatorname{Im}C_1
\end{aligned}
\tag{28}
$$

The function $\eta(\sigma,m)$ in expression of $\Psi(\zeta)$ is given by

$$
\eta(\sigma,m)=\frac{\mu_3(1+m)^2\chi^2(m\chi C_1+(2+\chi)\overline{C}_1)^2}{m^{3/2}(2+\chi-m\chi)^2(2+\chi+m\chi)^2}(1-m)^2\operatorname{arctanh}\left(\frac{\sigma}{\sqrt{m}}\right)
\tag{29}
$$

Since $(1-m)$ is a very small number and $|\sigma|=1$, Eq. (29) can be represented as

$$
\eta(\zeta,m)=\frac{4\mu_3\chi^2(\chi C_1+(2+\chi)\overline{C}_1)^2}{(2+\chi-\chi)^2(2+\chi+\chi)^2}(1+E_0(1-m))
\tag{30}
$$

where $E_0(1-m)$ represents a quantity far small than $(1-m)$, which can be neglected because it is far smaller than 1. By substituting Eqs. (27)–(30) into the fourth expression of Eq. (10), the displacements at a point on the crack surface can be expressed as

$$u_x(\sigma) + \mathrm{i}u_y(\sigma) = R(\gamma_1\sigma + \gamma_2\sigma^{-1}) \tag{31}$$

where

$$\begin{aligned} \gamma_1 &= \frac{(\kappa+1)A_1}{2G} - \frac{\mu_0(2\chi+1)\bar{c}_{-1}^2}{4Gm} + \frac{\mu_0(\overline{F}^2 m + 2F\overline{F})}{4G} \\ \gamma_2 &= \frac{(\kappa+1)a_{-1}}{2G} - \frac{\mu_0(2\chi+1)\overline{C}_1^2}{4G} + \frac{\mu_0(\overline{F}^2 + 2F\overline{F}m)}{4G} \end{aligned} \tag{32}$$

Since 2β is the maximum opening distance of the crack surface, it can be evaluated by the following inequality

$$|u_x(\sigma) + \mathrm{i}u_y(\sigma)| \leqslant \beta/\alpha < \sqrt{2}|u_x(\sigma) + \mathrm{i}u_y(\sigma)| \tag{33}$$

By substituting Eq. (32) into Eq. (33) and using Eq. (22) and the rule $|a+b| \leqslant |a| + |b|$, we obtain

$$(1-m) \leqslant \left|\frac{6(\kappa+1)p}{G}\right| + \left|\frac{9b_0^2/(\mu_0\chi)}{G}\right| \ll 1 \tag{34}$$

Since the tensile load, p, and the magnetic energy density of the material, $g_s = \frac{1}{2}b_{\mathrm{satur}}h_{\mathrm{satur}}$, are all much less than the elastic shear modulus, G, Eq. (34) substantiates that $(1-m)$ is a very small quantity in small deformation. The subscript "satur" denotes saturation quantities.

From Eq. (4), we obtain

$$z(\sigma) = u_x(\sigma) + \mathrm{i}u_y(\sigma) + (X + \mathrm{i}Y)_\sigma \tag{35}$$

where $(X + \mathrm{i}Y)_\sigma$ represents the position of a material point that moves to $z = g(\sigma)$ after deformation.

By means of the geometric analysis, the following relations can be obtained,

$$\begin{aligned} \max\{X^2 + Y^2\} &= \max_\sigma\{(x(\sigma) - u_x(\sigma))^2 + (y(\sigma) - u_y(\sigma))^2\} = a^2 \\ \min\{X^2 + Y^2\} &= \min_\sigma\{(x(\sigma) - u_x(\sigma))^2 + (y(\sigma) - u_y(\sigma))^2\} = 0 \end{aligned} \tag{36}$$

The maximum value of $\sqrt{X^2 + Y^2}$ is corresponding to $\sigma = \sigma_a$, which is the image of the crack tip position after deformation in the ζ-plane, i.e., $z_a = g(\sigma_a)$.

Since ϑ is the argument of the crack tip position in the Z-plane, $Z = \mathrm{e}^{-i\vartheta}(a + \mathrm{i}0)$, and by using Eqs. (35) and (36), three algebraic equations, which determine the geometric coefficients R, m and ϑ, are obtained.

$$\begin{aligned} &2R|1-\gamma_1| - a = 0 \\ &2R|m-\gamma_2| - a = 0 \end{aligned} \tag{37}$$

$$\vartheta + \arg(R(\sigma_a + m\sigma_a^{-1}) - R(\gamma_1\sigma_a + \gamma_2\sigma_a^{-1})) = 0$$

where

$$\sigma_a = \sqrt{\frac{(1-\bar{\gamma}_1)(m-\gamma_2)}{(1-\gamma_1)(m-\bar{\gamma}_2)}} \tag{38}$$

By solving Eq. (37), all the unknown coefficients, including R, m and θ, can be determined. Substitution of R, m and ϑ into Eqs. (10) and (28) leads to get the solution of the problem.

6. Coupling field near the crack tip

The stress and magnetic fields can be determined from Eqs. (5) and (10). These fields can be expressed as

$$\begin{aligned} t_{x'x'} + t_{y'y'} &= 2\left(\varphi'(z) + \bar{\varphi}'(\bar{z})\right) - v\mu_0\chi\omega'(z)\bar{\omega}'(\bar{z}) \\ t_{y'y'} - t_{x'x'} + 2\mathrm{i}t_{x'y'} &= \mathrm{e}^{2\mathrm{i}\vartheta}\left(2\left(\bar{z}\varphi''(z) + \psi'(z)\right) + (1-v)\mu_0\chi\omega''(z)\bar{\omega}(\bar{z}) - \mu_0\chi\omega'(z)^2\right) \\ h_{x'} - \mathrm{i}h_{y'} &= \exp(-\mathrm{i}\vartheta)\omega'(z) \end{aligned} \tag{39}$$

The displacement field is given by

$$(U_{X'} + \mathrm{i}U_{Y'}) = \tfrac{1}{2}G^{-1}\mathrm{e}^{\mathrm{i}\vartheta}(\kappa\varphi(z) - z\bar{\varphi}'(\bar{z}) - \bar{\psi}(\bar{z}) - \tfrac{1}{2}(1-v)\mu_0\chi\omega(z)\bar{\omega}'(\bar{z})) \tag{40}$$

From Eqs. (10) and (27), we obtain the stress field at the crack tip as follows:

$$\begin{aligned} t_{yy} + \mathrm{i}t_{xy} = &\frac{A_1 - \mathrm{e}^{-2\mathrm{i}\theta_a}a_{-1}/R}{1 - m\mathrm{e}^{-2\mathrm{i}\theta_a}} + \frac{(1-v)\mu_0\chi(C_1 - c_{-1}\mathrm{e}^{-2\mathrm{i}\theta_a})(\overline{C}_1 - \bar{c}_{-1}\mathrm{e}^{-2\mathrm{i}\theta_a})}{2(1 - m\mathrm{e}^{-2\mathrm{i}\theta_a})(1 - m\mathrm{e}^{2\mathrm{i}\theta_a})} \\ &- \frac{\mu_0(2\chi+1)(C_1 - c_{-1}\mathrm{e}^{-2\mathrm{i}\theta_a})^2}{2(1 - m\mathrm{e}^{-2\mathrm{i}\theta_a})} - \frac{\mu_0 F^2}{2} \end{aligned} \tag{41}$$

The magnetic field at the crack tip is given by

$$h_x - \mathrm{i}h_y = (C_1 - c_1\mathrm{e}^{-2\mathrm{i}\theta_a})/(1 - m\mathrm{e}^{-2\mathrm{i}\theta_a}) \tag{42}$$

where θ_a is the argument σ_a. The results show that the stress and magnetic fields at the crack tip are very large. However, they are finite in the deformed configuration. To determine the field near the crack tip, defining that

$$z = z_a + r\mathrm{e}^{\mathrm{i}\theta} \tag{43}$$

where r is the distance from the crack tip, and $r \ll a$. z_a is the deformed crack tip position; and θ is the angle from the line oz_a to the r-direction. From Eq. (39), the inverse function of Eq. (21) and the second and third expressions of Eq. (37), the magnetic field can be obtained as follows:

$$h_{x''} - \mathrm{i}h_{y''} = C_1 + \frac{\frac{1}{2}(1-m)(1+\chi)(C_1 - \overline{C}_1)z_a}{\sqrt{2ar\mathrm{e}^{\mathrm{i}\theta} - (z_a^2 - a^2) - (m\gamma_1 + \gamma_2 + \gamma_1\gamma_2)}} \tag{44}$$

The magnetic field in the ring region where $a \gg r \gg \beta$ can be expressed as

$$h_{x''} + \mathrm{i}h_{y''} = \frac{k_{\mathrm{mag}}}{\sqrt{r}}\mathrm{e}^{-\mathrm{i}\theta/2} \tag{45}$$

and

$$k_{\mathrm{mag}} = \frac{c_{\mathrm{eff}}(\overline{C}_1 - C_1)\sqrt{a}}{2\sqrt{2}} \tag{46}$$

where

$$c_{\mathrm{eff}} = (1-m)(1+\chi) \tag{47}$$

For materials with small relative permeability (for example, most of steels usually has a relative permeability of $\chi = 10$), the factor $c_{\mathrm{eff}} = (1-m)(1+\chi)$ is very small. Magnetic concentration occurs in a very small region near the crack tip. The maximum value of distance r is as small as the coefficient, β. On the other hand, for materials with a large χ, for instance, $\chi = 2 \times 10^4$, the factor c_{eff} is not very small. The region of magnetic concentration overlaps with the region of the local stress field.

The local stress field in the ring region ($a \gg r \gg \beta$) near a crack tip characterizes linear elastic fracture. It can be seen that the difference between z_a and $z = a$ is a higher-order quantity that is smaller than in this region. From Eqs. (39) and (21), the stress in the region can be expressed as

$$t_{y''y''} + \mathrm{i}t_{x''y''} = \frac{\sqrt{\frac{1}{2}a}(A_1 - a_{-1}/R)}{\sqrt{r}}\mathrm{e}^{\mathrm{i}\theta/2} - \frac{\mu_0(1+v)\chi|C_1 - \overline{C}_1|^2 a(1-m)^2(1+\chi)^2}{16r}\mathrm{e}^{\mathrm{i}\theta} \tag{48}$$

It is obvious that the stress field consists of $r^{-1/2}$ and r^{-1} terms, which is the result obtained from the constitutive relations given by Eq. (5). In this equation, the stress field is associated with the product of magnetization and magnetic intensity.

7. Discussions

7.1. Deformed crack surface

In Section 3, the deformed crack surface has been assumed to be an elliptical cylinder. From the results obtained by using Eqs. (27), (30) and (31), it can be seen that the deformed crack surface is an elliptical cylinder when a high-order quantity that is smaller than $(1 - m)$ is neglected. The assumption made for the deformed crack surface will be validated as follows:

From the fourth expression of Eq. (10) and Eqs. (27) and (30), the error of the displacements expressed by Eq. (31) can be estimated as follows:

$$E_u = (u_x + \mathrm{i}u)_y - R(\gamma_1\sigma + \gamma_2\sigma^{-1}) = \gamma_3 E_0(1-m) \tag{49}$$

where

$$\gamma_3 = \frac{\mu_0(2\chi+1)(1+m)^2\chi^2\overline{C}_1^2(m\chi C_1 + (2+\chi)\overline{C}_1)^2}{4Gm^{3/2}(2+\chi-m\chi)^2(2+\chi+m\chi)^2} \tag{50}$$

This shows that the error, E_u, arising from Eq. (31) is far less than $(1 - m)$.

Moreover, the effect of the very small error on magnetic field can be also negligible. Assuming that the projected curve of the crack surface γ is more complex than an ellipse and it can be expressed by conformal transformation

$$z = R(\zeta + \lambda_1\zeta^{-1} + \lambda_5\zeta^{-5}), \quad \zeta = \sigma = \mathrm{e}^{\mathrm{i}\theta} \tag{51}$$

where λ_1 and λ_5 are two real constants. It can be determined from Eq. (50) that λ_5 is as small as $(1 - m)$. By using Eq. (51), the magnetic field can be determined from the first two expressions of Eqs. (15) and (18). Thus, we obtain

$$W(\zeta) = (RC_1\zeta + Rc_1\zeta^{-1}) + \lambda_5 c^*_{-5}\zeta^{-5} + \lambda_5^2 f(\zeta) + \cdots \tag{52}$$

where

$$c^*_{-5} = \frac{\mu_b(\lambda_1(1+\lambda_1^4)(\mu_b^2-1)\overline{C}_1 + ((1+\lambda_1^6)(1+\mu_b^2) + 2(1-\lambda_1^6)\mu_b)C_1)}{(1+\lambda_1+(1-\lambda_1)\mu_b)(1-\lambda_1+(1+\lambda_1)\mu_b)(1+\lambda_1^5+(1-\lambda_1^5)\mu_b)(1-\lambda_1^5+(1+\lambda_1^5)\mu_b)} \tag{53}$$
$$\mu_b = (1+\chi_-)/(1+\chi)$$

Eq. (52) shows that the error of the magnetic field also is a high-order term of a small quantity. Thus, the deformed crack surface of a magnetoelastic problem can be regarded as an elliptical cylinder. It is interesting to note that the projected curve of the deformed crack in the adopting linear constitutive relations can be deduced to be an exact ellipse.

Table 1
The solution of α and β for the case of $\theta_b = 0°$, $b_0 = 0.94$ T

p	0 Pa	0.1 MPa	1 MPa	10 MPa	20 MPa	50 MPa	70 MPa	90 MPa
α/a	1.00000	1.000002	1.000004	1.00002	1.00005	1.00011	1.00018	1.00023
β/a	3e−015	4.6390e−8	3.016e−7	2.853e−5	5.689e−5	1.4198e−4	1.9872e−4	2.5547e−4

Table 2
The solution of ϑ for different direction of mechanical tension

p	0 Pa	1 MPa	10 MPa	20 MPa	40 MPa	50 MPa	70 MPa	90 MPa
$\theta_p = 90°$	2e−28	−1e−21	2e−22	−6e−22	1e−21	3e−21	2e−21	5e−21
$\theta_p = 80°$	−6.3e−11	−8.43e−8	−8.44e−7	−1.68e−6	−3.37e−6	−4.21e−6	−5.90e−6	−7.59e−6
$\theta_p = 60°$	5.8e−11	−2.13e−7	−2.13e−6	−4.27e−6	−8.54e−6	−1.06e−5	−1.49e−5	−1.92e−5

Consider a material of Young's modulus $E = 200$ GPa, $v = 0.3$, $\chi = 70$ with a crack of length $2a = 0.1$ m. The homogeneous magnetic field is gotten in terms of $b_0 = 0.003\sqrt{\mu_0 G} = 0.94$ T, $\theta_b = 0°$ and $\theta_p = \mathbf{0}$. The results of α and β for different values of p are presented in Table 1. The material inside the deformed crack is assumed to be air. The data show that the coefficient α is very close to a; and β is a very small quantity. The value of β increases with increasing p. For $p = 70$ MPa, β is about 25.5 μm, which is much larger than that of 0.3 μm for $p = 1$ MPa. Table 2 presents the values of ϑ for different p and direction θ_p. It can be seen from the table that the angle between the symmetric axes of the deformed and undeformed crack surfaces is very small.

7.2. The magnetic field near the crack tip

The results obtained in Section 6 show that the magnetic field is concentrated near the crack tip. In the region of $\beta \ll r \ll \alpha$, the magnetic field is governed by $1/\sqrt{r}$. The factor of the magnetic field concentration, K_{mag}, is plotted against the mechanical tension for different susceptibilities, as shown in Fig. 2. In this example of the plane stress problem, $h^\infty = 80$ A/m, $E = 200$ GPa, $v = 0.3$, $\chi_- = 0$ and $\theta_p = \theta_b = 0$. The

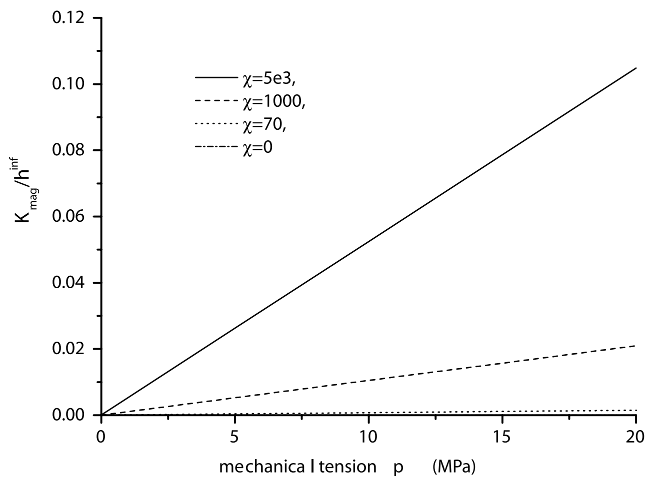

Fig. 2. Relations of the magnetic-field concentration coefficient (K_{mag}) vs. mechanical loading (f) for the cases with different material susceptibility χ.

results show that the magnetic concentration is influenced by both the magnetic susceptibility and mechanical tension.

Based on the stress field given by Eq. (44), the saturation region can be estimated by

$$\left| C_1 + \frac{\frac{1}{2}(1-m)(1+\chi)(C_1 - \overline{C}_1)z_a}{\sqrt{2are^{i\theta} - (z_a^2 - a^2) - (m\gamma_1 + \gamma_2 + \gamma_1\gamma_2)}} \right| \geqslant \frac{M_s}{\chi} \tag{54}$$

The estimated radius of the saturation region is given by

$$r \leqslant r_s = \left(\frac{c_{\text{eff}} b_y^\infty}{\sqrt{2}(b_{\text{satur}} - b^\infty)} \right)^2 a \tag{55}$$

where b_{satur} is the saturation magnetic flux density of the material; and b^∞ is the value of the magnetic induction in the homogeneous field.

Eq. (55) implies that the size of magnetic saturation is affected by the deformation, the magnetic susceptibility and the applied magnetic field in the direction normal to the crack. Consider an example in which the material constants are $G = 78$ GPa, $v = 0.3$, $b_{\text{satur}} = 1.7$ T and the material is subjected to a homogeneous field of $\sigma_{xx}^\infty = 7.8$ MPa, $\sigma_{xx}^\infty = \sigma_{xy}^\infty = 0$, $b_x^\infty = 0$. For different magnetic susceptibilities of the material, the relation between the radius of the saturation region, r_s, and b_y^∞ are shown in Fig. 3. It can be seen that the radius of the saturation region increases with increasing b_y^∞ in the range below b_{satur}. Moreover, the higher the magnetic susceptibility, the larger is the size of the saturation region.

7.3. The stress field near the crack tip

From Eq. (48), stress near the crack tip is contributed by the two items. The first item proportion to $\sqrt{r}$ and the second one to r. Correspond to this, two factors k_{item1} and k_{item2} is used. The stress for a material of $G = 78$ GPa, $\chi = 500$ and $v = 0.3$ is calculated. k_{item1}, k_{item2} and k_{linear} which is the stress singularity factor by using linear model are shown in Fig. 4. The homogeneous field are $\sigma_{yy}^\infty = 1$ MPa, $\sigma_{xx}^\infty = \sigma_{xy}^\infty = 0$, $b_x^\infty = 0$ and $b_y^\infty = 0.2$ T. It can be seen from the figure that k_{item1} varies slowly with the applied magnetic field increased. The factor calculated by using linear model, k_{linear}, has a singularity value when the denominator equal to zero (Liang et al., 2000). k_{item2} reflects the magnetic pull between the crack surfaces. The item is negative

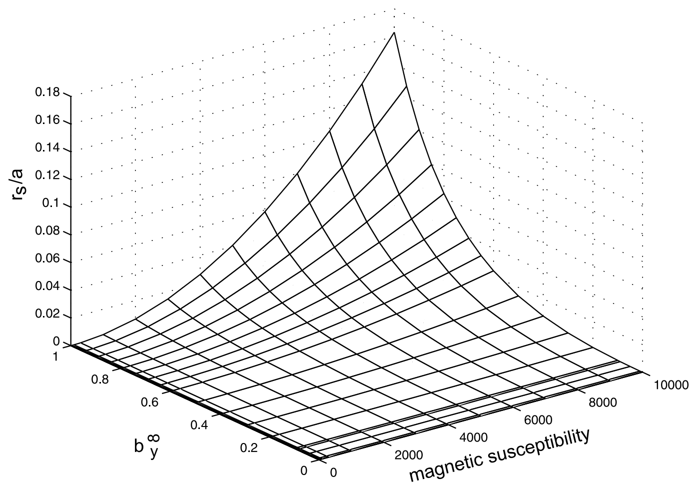

Fig. 3. The radius of magnetic saturation region, r_s, under different b_y^∞ and material susceptibility χ.

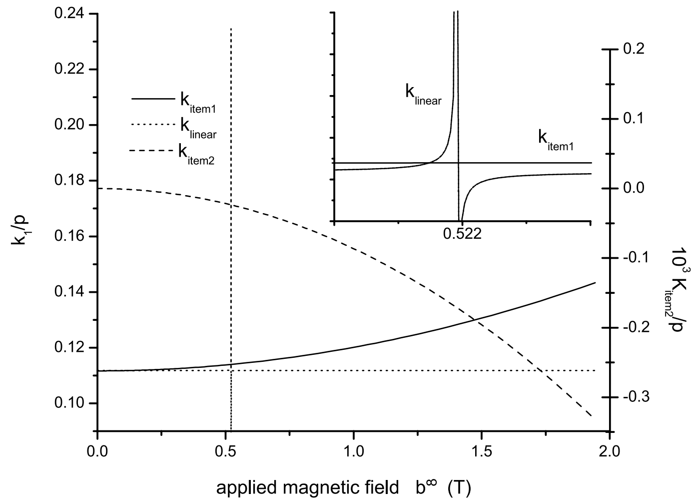

Fig. 4. The factor of stress singularity on the crack tip for a material of $\chi = 500$.

which reduces is the stress concentration near the crack tip. Fig. 4 shows that the absolute value of k_{item2} is increased with the magnetic induction on the material enhancing.

In the case where the material has small relative magnetic permeability, c_{eff} is a small quantity. The magnetic saturation region is as small as the yield region. The concept of small scale yielding in linear elasticity can be adopted. In this case fracture is governed principally by the local stress in region where $\beta \ll r \ll \alpha$. In the case where the material has large relative permeability, the stress field is complicated. The saturation region is not very small and the stress expression has an item that is proportion to r^{-1}.

The stress field for materials with different magnetic permeability is calculated. In this example, a homogeneous far field where $\sigma_{yy}^{\infty} = 30$ MPa, $\sigma_{xx}^{\infty} = \sigma_{xy}^{\infty} = 0$, $b_x^{\infty} = 0$ and $b_y^{\infty} = 1$ T, is applied to the material. The material inside the deformed crack is assumed to be air. The relation between the normalized stress, $\sigma_{yy}/\sigma_{yy}^{\infty}$, and the distance from the crack tip r, is shown in Fig. 5. The solid curve represents stress for a

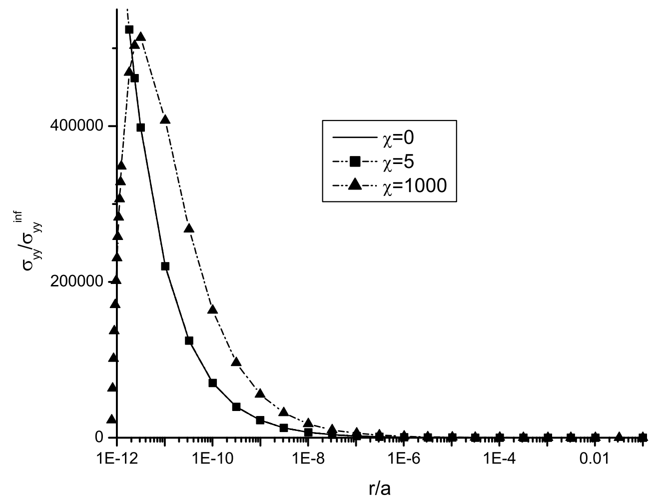

Fig. 5. The stress, σ_{yy}, in the front of the crack vs. the distance from crack tip.

noncoupling problem is also presented. The curve with a rectangle is corresponding to a material of $E = 200$ GPa, $v = 0.28$, $\chi = 5$ and the one with a triangle is for $E = 70$ GPa, $v = 0.28$, $\chi = 1000$. It can be seen that the curves for $\chi = 5$ and the result of noncoupling are almost identical. This shows that the effect of magnetoelastic coupling on fracture for materials with small magnetic susceptibility is very small. Fig. 5 also shows that the stress for $\chi = 1000$ is obviously difference from the result of noncoupling. The magnetoelastic coupling influence the stress field near the crack tips for a ferromagnetic material of large susceptibility and small stiffness.

8. Conclusions

The magnetoelastic problem of an infinite plate with a crack is studied in this paper. The magnetic and stress fields can influence the fracture of soft ferromagnetic materials. The magnetic field is concentrated near the crack tip. The magnetic saturation region near the crack tip is estimated, whose size is related to the material constants and the deformed crack surface. The effect of cracking on the concentration of magnetic field is related to the deformed crack surface and the material constants. The magnetic effect on fracture of materials with small susceptibility is not obvious. Clatterbuck et al. (2000) had performed an experiment on a material of low magnetic susceptibility. The experimental results show that magnetic field does not have obviously effect on the fracture of the material tested, which result is agree with the calculations made in this paper. However, there is insufficient ferromagnetic fracture data to examine crack initiation and/or propagation. Further experimental work and dynamic problem of soft ferromagnetic materials is in progress.

Acknowledgements

Support from the National Science Foundation of China (no. A020206), from the China Postdoctoral Science Foundation and from the Research Grants Council of the Hong Kong Special Administrative Region, China (project no. HKU 7063/01E) is acknowledged.

References

Bagdasarian, G.Y., Hasanian, D.J., 2000. Magnetoelastic interaction between a soft ferromagnetic elastic half-plane with a crack and a constant magnetic field. Int. J. Solid Struct. 37, 5371–5383.

Brown Jr., W.F., 1966. Magnetoelastic Interactions. Springer-Verlag, New York.

Clatterbuck, D.M., Chan, J.W., Morris, J.M., 2000. The influence of a magnetic field on the fracture toughness of ferromagnetic steel. Mater. Trans. JIM 41, 888–892.

Eringen, A.C., 1980. Mechanics of Continua, second ed. Krieger Publishing, New York.

Eringen, A.C., 1989. Theory of electromagnetic elastic plates. Int J. Eng. Sci. 27, 363–375.

Knops, J.R., 1963. Two-dimension electrostriction. J. Mech. Appl. Math., 377–388.

Liang, W., Shen, Y., Zhao, M., 2000. Magnetoelastic formulation of soft ferromagnetic elastic problems with collinear cracks: energy density fracture criterion. Theor. Appl. Fract. Mech. 34, 49–60.

Maugin, G.A., 1988. Continuum Mechanics of Electromagnetic Solids. Amsterdam, North-Holland.

McMeeking, R.M., 1999. Crack tip energy release rate for a piezoelectric compact tension specimen. Eng. Fract. Mech. 64 (2), 217–244.

McMeeking, R.M., 2001. Towards a fracture mechanics for brittle piezoelectric and dielectric materials. Int. J. Fract. 108 (1), 25–41.

Moon, F.C., 1984. Magneto Solid Mechanics. John Wiley & Son Inc., New York.

Pao, Y.H., Yeh, C.S., 1973. A linear theory for soft ferromagnetic elastic solids. Int. J. Eng. Sci. 11, 415–436.

Sabir, M., Maugin, G.A., 1996. On the fracture of paramagnets and soft ferromagnets. Int. J. Non-Linear Mech. 31, 425–440.

Shindo, Y., 1977. The linear magnetoelastic problem for a soft ferromagnetic elastic solid with a finite crack. ASME J. Appl. Mech. 44, 47–50.
Shindo, Y., 1980. Singular stress in a soft ferromagnetic elastic solid with two coplanar Griffith cracks. Int. J. Solid Struct. 46, 537–543.
Shindo, Y., Ohnishi, I., Tohuama, S., 1997. Flexural wave scattering at a though crack in a conducting plate under a uniform magnetic field. J. Appl. Mech. 64, 828–834.
Shindo, Y., Ohnishi, I., Toyama, S., 2000. Dynamic singular moments in a perfectly conducting mindlin plate with a through crack under a magnetic field. J. Appl. Mech.-T. ASME 67 (3), 503–510.
Sosa, H., Khutoryansky, N., 1996. New developments concerning piezoelectric materials with defects. Int. J. Solids Struct. 33 (23), 3399–3414.
Wohlfarth, E.P., 1980. Ferromagnetic Materials. North-Holland Publishing Company, Amsterdam.
Yeh, C.S., 1989. Magnetic fields generated by a mechanical singularity in a magnetized elastic half plane. ASME J. Appl. Mech. 56, 89–95.
Yerma, P., Singh, M., 1984. Finite deformation theory for soft ferromagnetic elastic solids. Int. J. Non-Linear Mech. 19 (4), 273–286.
Zhang, T.Y., 1998. Energy release rate for a crack or a cavity in a piezoelectric material. Key Eng. Mater. 145–149 (2), 1021–1030.
Zhang, T.Y., Qian, C.F., Tong, P., 1998. Linear electro-elastic analysis of a cavity or a crack in a piezoelectric material. Int. J. Solids Struct. 35 (17), 2121–2149.